

SOME PHYSICAL CHARACTERISTICS OF MICROCRYSTALLINE CELLULOSE

1. POWDERS FOR PHARMACEUTICAL USE

Keith Marshall and David Sixsmith

Industrial Pharmacy Unit, Postgraduate School of Studies in
Pharmacy, University of Bradford, Bradford, Yorkshire
BD7 1DP, England.

ABSTRACT

Four grades of commercially available microcrystalline cellulose have been examined and the appearance, particle size distributions, specific surface areas, pore size distributions and surface energies determined. The median Stokes diameters show general correlation with published data, but Coulter counter results are larger by a factor of approximately 1.4. Correlation is also seen with values obtained from air permeametry experiments.

Scanning electron-microscopy demonstrated the presence of two general types of particle, one roughly rod-like and the other an irregular mass. At higher magnifications, fully hydrolysed samples show a microfibrillar structure, the individual fibrils possessing a transparent longitudinal axis. The possibility that the fibrils are hollow is confirmed by analysis of the adsorption isotherms using mathematical models which indicate that the materials are porous, with a modal radius value of about 2.0 nm.

MARSHALL AND SIXSMITH

Interparticulate voids with modal radii ranging from 5 μ m to 35 μ m, dependent on the grade examined, were found from high pressure Mercury Intrusion Porosimetry. No significant differences in specific surface energy were detected from the heats of adsorption using a flow microcalorimetric technique, suggesting that the surface forces in all four grades are of a similar magnitude.

INTRODUCTION

Amongst the reasons for the pharmaceutical popularity of microcrystalline cellulose are its attractive compaction⁽¹⁾ and disintegration characteristics⁽²⁾. Both these properties have been attributed to the presence of hydrogen bonds between the particles⁽²⁾, and such bonds have recently been demonstrated⁽³⁾.

A lack of quantitative information in the literature led to the decision to investigate those properties which might contribute to the compaction qualities of some commercially available microcrystalline celluloses, namely the 'Avicels' (FMC Export Corpⁿ., Penn., U.S.A.). Physical properties related to the surface characteristics such as surface energy, surface area, particle size and pore structure might be anticipated to affect behaviour under compressive forces and therefore received consideration first. The preliminary work has already been reported⁽⁴⁾ and the present paper concerns the detailed examination of single batches of four grades of Avicel, (PH 101, PH 102, PH 103 and PH 105) as received, except that where appropriate, measurements were carried out in a controlled environment room (20°C and 35 to 40% RH), after conditioning

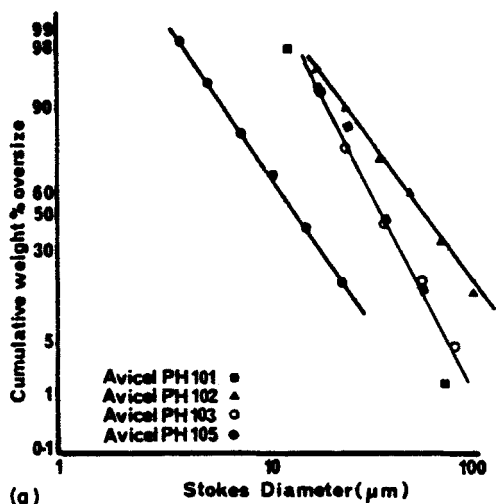
the samples in it for several days. Samples were obtained from the bulk by means of a spinning riffler (Microscal, London).

EXPERIMENTAL

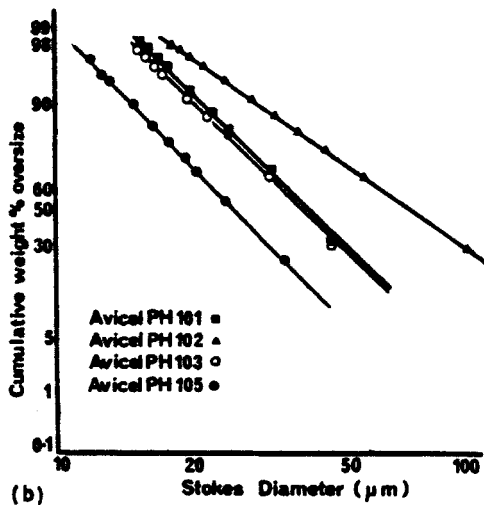
Determination of Particle Size Distributions

The size distributions and median Stokes diameters were determined by gravitational sedimentation in distilled water, or where appropriate in a 50% v/v glycerin solution at 20°C. Suspension concentrations of about 0.05% w/v were used and no dispersing agent was found to be necessary. The instruments used were an E.E.L. photosedimentometer (Evans Electro-Selenium Ltd., Harlow) and a W.A.S.P. photosedimentometer (Microscal Ltd., London), but the scanning facility of the latter instrument was not used. The results from the W.A.S.P. recorder give a measure of size distribution in relation to surface area, but this was also converted to a size distribution by weight, for comparison with data from the E.E.L. and that quoted in the literature. Typical results are shown in Figure 1(a) and 1(b) and summarised in Table I.

Size distributions were also obtained using a Model "T" Coulter Counter (Coulter Electronics Inc., Hialeah) by suspending the Avicels in 1.0% Sodium Chloride solution as electrolyte. Because of the wide range of particle size present a two-tube technique was necessary with all samples except PH 105. The results of these analyses are also summarised in Table I and typical distributions illustrated in Figure 1(c).



(a)



(b)

FIGURE 1.

Cumulative Weight Size distributions determined by (a) E.E.L. photosedimentometer (b) W.A.S.P. photosedimentometer (c) Coulter Counter.

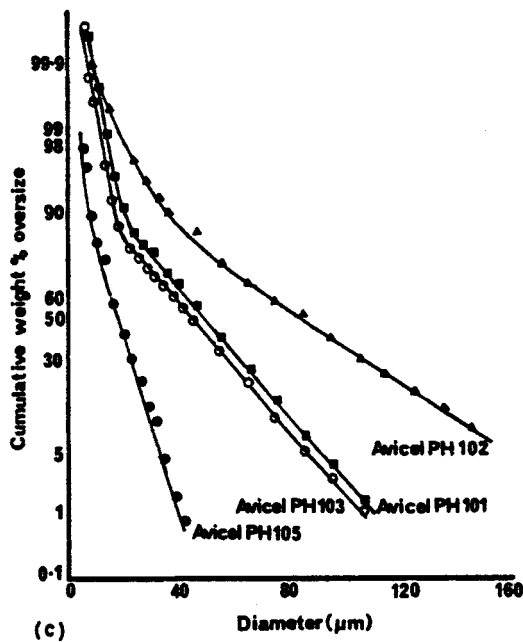


Fig. 1 (continued)

Permeametry

An air permeametry apparatus (Fisher Sub-sieve Sizer, KEK Ltd., Manchester) was used to determine a median diameter and derived surface area for each of the conditioned powders at porosities, ' ϵ ', between 0.80 and 0.60. In each instance a minimum median size was reached within this range ($\epsilon = 0.65$), the values in Table I being the arithmetic means of four such experiments.

Surface Area Determinations

Surface areas were determined by Nitrogen adsorption at -196°C using a standard gas adsorption apparatus⁽⁶⁾ with liquid Nitrogen

TABLE I
Geometric Properties of Avicels

	AVICEL PH GRADE:			
	102	101	103	105
Median Diameter* (μm)	90	37	37	-
W.A.S.P. Median Stokes diameter by surface (μm)	47	35	34	18
Median Stokes diameter by weight (μm)	62	37	36	25
Surface Area ($\text{m}^2 \text{g}^{-1}$)	0.06	0.11	0.11	0.16
E.E.I. Median Stokes diameter by weight (μm)	52	33	33	13
Surface Area ($\text{m}^2 \text{g}^{-1}$)	0.08	0.12	0.12	0.31
Permeametry Median Diameter (μm)	16.0	15.3	15.3	6.3
Surface Area ($\text{m}^2 \text{g}^{-1}$)	0.25	0.26	0.26	0.63
Coulter Counter Median Diameter (μm)	85.5	49.5	46	16.5
Surface Area ($\text{m}^2 \text{g}^{-1}$)	0.05	0.08	0.09	0.24
Gas Adsorption B.E.T. ($\text{m}^2 \text{g}^{-1}$)	10.0	11.2	11.4	20.7
Huttig ($\text{m}^2 \text{g}^{-1}$)	10.5	11.4	11.5	22.0

* Avicel Technical Literature (5)

as the coolant. Approximately 1.0g of sample of each grade, corresponding to 10 to 20 m^2 of surface, was degassed at 100 to 110°C and a pressure less than 0.15 N m^{-2} .

MICROCRYSTALLINE CELLULOSE. 1

A preliminary study of measured surface area against time of degassing had shown that a constant surface area value was only reached after about 8 hours degassing, see Figure 2. Therefore all samples were allowed to degas overnight, normally 12 to 14 hours, before being analysed. The mean results of three of these experiments for each powder are also summarised in Table I.

Mercury Intrusion Porosimetry

The mercury penetration volume at various intrusion pressures was measured using a mercury penetration porosimeter (Model 905-1, Micromeritics Inst. Corp., Norcross). For each determination approximately 0.5g of powder was introduced into the sample cell and this was placed in the pressure chamber.

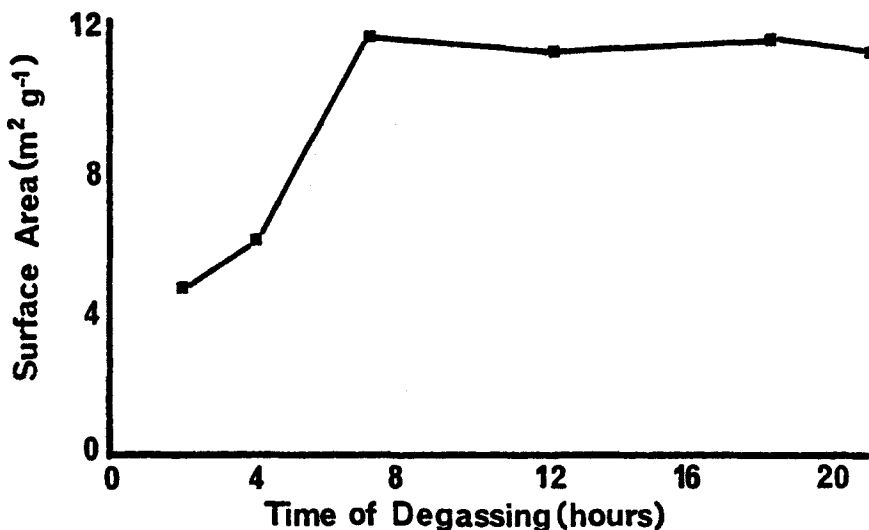


FIGURE 2.

Effect of time of degassing on the B.E.T. surface area for Avicel PH 101.

MARSHALL AND SIXSMITH

The cell and sample were degassed and then mercury allowed to enter until the cell was full. The pressure was increased and the volume of mercury penetrating the powder at each pressure determined by the volume of mercury in the sample holder. The pressure was increased up to a maximum of 280 MN m^{-2} , those pressures above atmospheric being applied hydraulically.

The pore size distributions were calculated assuming a surface tension value for mercury of 0.474 N m^{-1} and a contact angle with the microcrystalline celluloses of 130° . Specimen results are shown graphically in Figure 3.

Microcalorimetry

The adsorption of solutions of n-butanol in n-heptane was studied using a flow microcalorimeter (Microscal Ltd., London). All the powders used were dried at $80\text{--}90^\circ\text{C}$ and cooled in a desiccator prior to use. The n-heptane was purified by passage through a silica gel column.

The heats of adsorption at monolayer coverage were determined using a continuous flow technique⁽⁷⁾.

Electron Microscopy

The untreated powders were almost too dense for conventional electron microscopy therefore scanning electron photomicrographs were taken at magnifications of 200 to 500 times using a Stereoscan 600 microscope (Cambridge Scientific Instruments Ltd., Cambridge), see Figure 4. In addition, samples of powder were treated by boiling in 4 N Acetic Acid for 8 hours to completely hydrolyse

MICROCRYSTALLINE CELLULOSE. 1

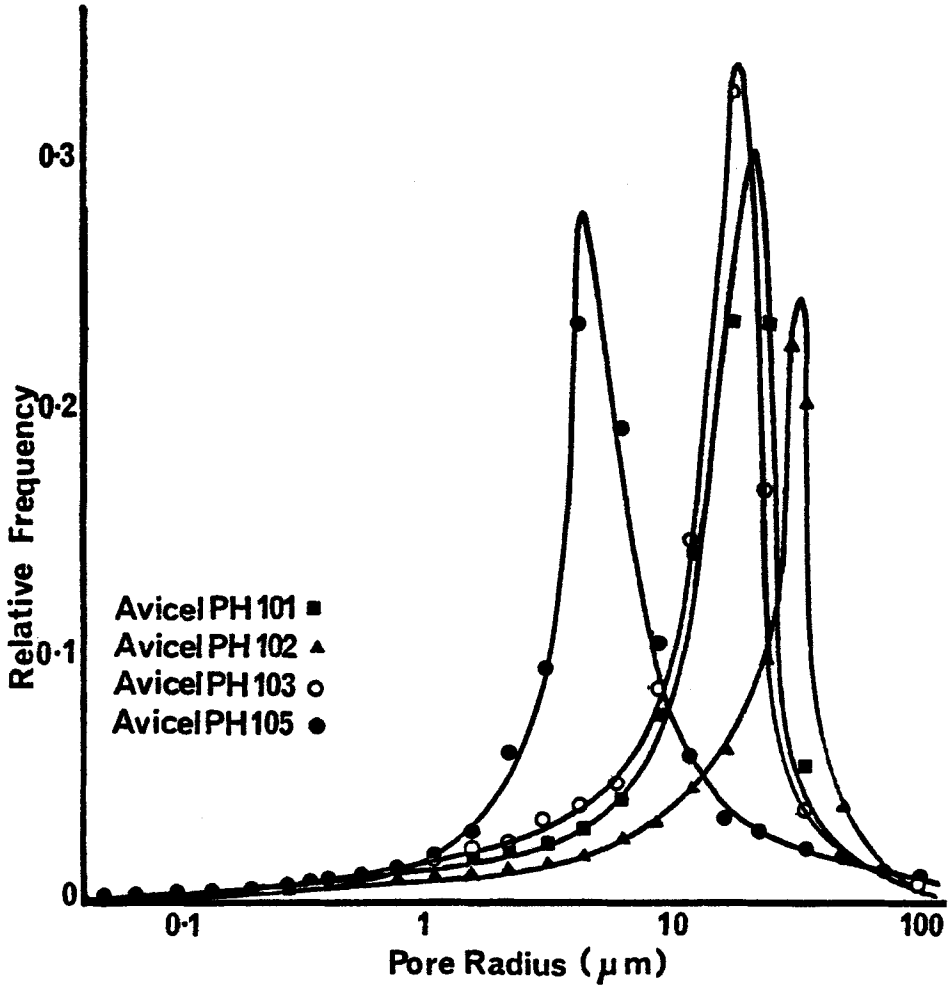


FIGURE 3.

Inter particulate pore size distributions for microcrystalline celluloses.

them. They were then washed in distilled water until acid free and examined microscopically using an AEI EM6B electron microscope

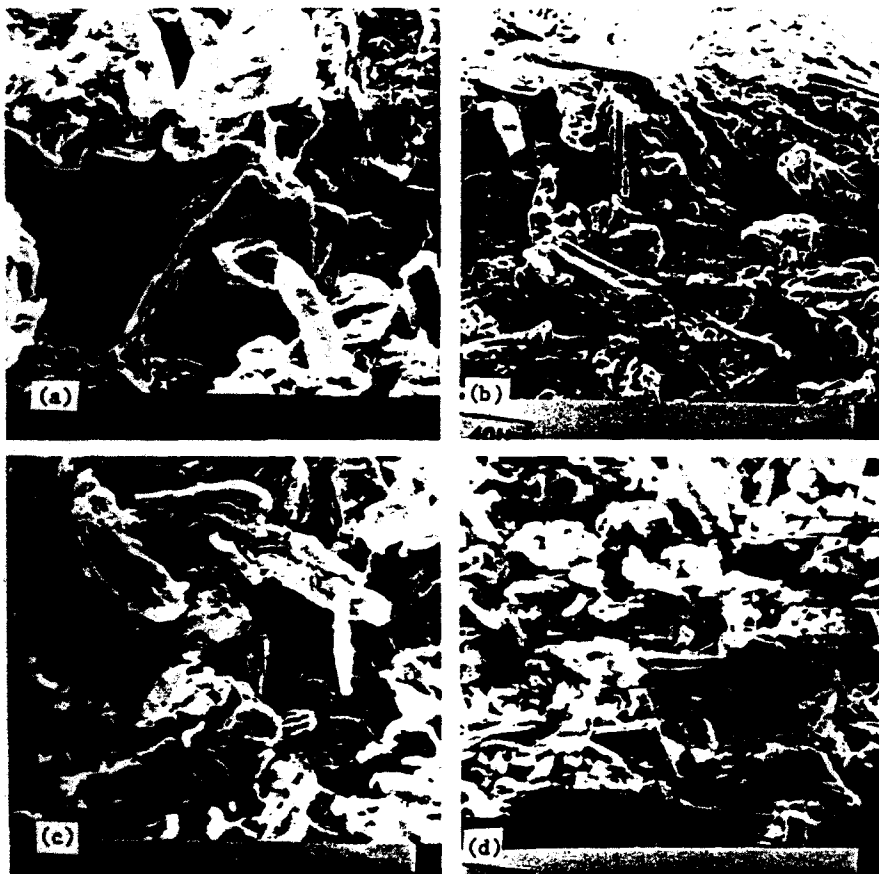


FIGURE 4.

Stereoscan photomicrographs of the four grades of microcrystalline cellulose (a) Avicel PH 101 (b) Avicel PH 102 (c) Avicel PH 103 (d) Avicel PH 105.

(AEI, Harlow) at magnifications between 150,000 and 500,000 times.

At a later stage untreated samples were also examined at similar magnifications, in some cases phosphotungstic acid was used to

MICROCRYSTALLINE CELLULOSE. 1

'dye' the observed internal capillaries of the fibrils. Typical electron photomicrographs of each type are shown in Figure 5.



FIGURE 5.

Electron photomicrographs of (a) Treated (b) Untreated samples of microcrystalline cellulose.

RESULTS AND DISCUSSION

From Table I it can be seen that the median Stokes diameters obtained from sedimentation show rank order correlation with those quoted by the manufacturers, but the Coulter counter results consistently gave higher values leading to a compensating shape factor of about 0.73.

The surface areas calculated from these results using the relationship

$$\text{Specific Surface Area} = \frac{6 \times 10^6}{\bar{d} \cdot \rho} \quad \text{m}^2 \text{ g}^{-1}$$

(where \bar{d} is the median diameter in μm and ρ is the density of the material)

were of the order of 0.06 to 0.6 $\text{m}^2 \text{ g}^{-1}$ and in view of the very different techniques involved again showed good rank order correlation with those from the permeametric measurements.

The probability/size graphs shown in Figures 1(a) and 1(b) for Stokes diameter suggest that the size distribution is logarithmically normal, whilst those for equivalent volume diameters indicate a normal distribution, Figure 1(c). In addition, there is a change in slope of the latter curves which is indicative of a mixed population of particles. Plotting the results obtained from the adsorption experiments in the normal manner showed that all four grades of powder gave Type II isotherms as seen in Figure 6. Applying the B.E.T. (8) and Huttig (9) equations to these isotherms enabled the surface areas to be determined (Tables I and II). Comparison of these values with the derived

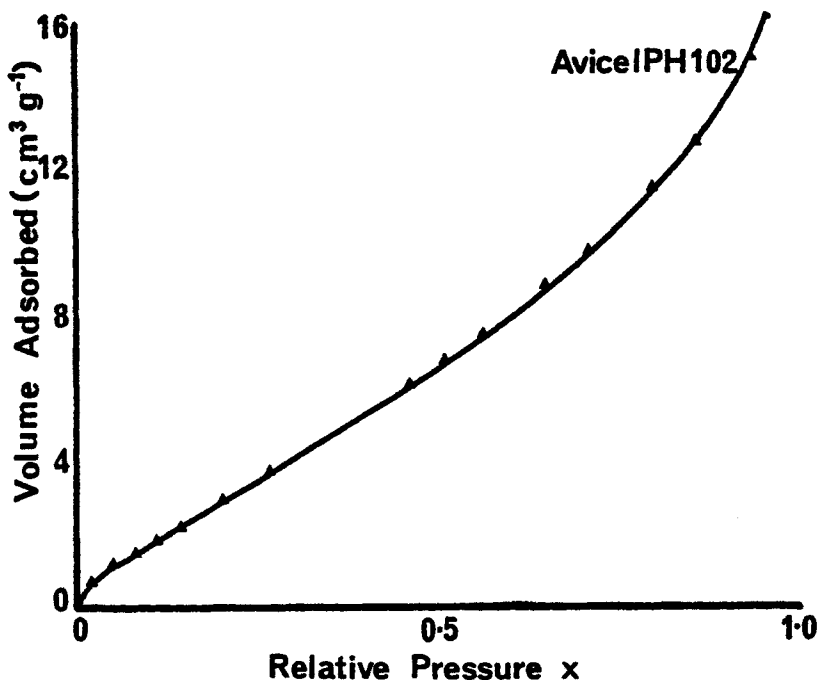


FIGURE 6.

Adsorption isotherm for microcrystalline cellulose.

values obtained from the Stokes diameters indicates that even if account is taken of the large differences in methodology the surface area being measured by Nitrogen adsorption is much greater than just the external surface of the particles.

It has been argued⁽¹⁰⁾ that a plot of volume of gas adsorbed ' V_a ' against statistical thickness of the adsorbed layer ' t ' will be a straight line passing through the origin, provided the gas is allowed to adsorb on to the surface unimpeded. If, however, adsorption is hindered, e.g. by pores in the surface, the gradient

MARSHALL AND SIXSMITH

of the $V_a - t$ plot will change and then remain at a new constant value, until the gas is again allowed to adsorb unimpeded, as would be the case when the pores became filled. From the values at the points of inflexion it is possible to calculate the approximate range within which the majority of pore radii lie, by applying Kelvin's equation⁽¹¹⁾. This relates the pore radius ' r_k ' which will be completely filled by the adsorbed nitrogen at a given pressure, P , relative to the vapour pressure of the bulk adsorbate P_o .

$$\text{i.e. } \log_e \frac{P}{P_o} = - \frac{2 \sigma \bar{V}}{r_k RT} \quad \text{----- (1)}$$

where ' σ ' is the surface tension and \bar{V} the molar volume of the adsorbing gas. For liquid Nitrogen equation (1) reduces to:-

$$\log_e \frac{P}{P_o} = - \frac{4.1}{r_k} \quad \text{----- (2)}$$

Subjecting the isotherms of each sample to such an analysis produced the results shown in Figure 7, suggesting that the powders were indeed porous, and had a majority of pores with radii between 1.0 and 5.0 nm, corresponding to ' t ' values of 0.35 and 0.85 from Figure 7.

Mathematical models based on Kelvin's equation⁽¹¹⁾ have been derived to enable the surface area of porous solids to be calculated, by assuming pores of either cylindrical or parallel plate cross-section. A correction factor is introduced with these models to allow for the thickness of the adsorbed layer, i.e. statistical thickness on the pore wall, ' t_s ' so that the corrected

MICROCRYSTALLINE CELLULOSE. 1

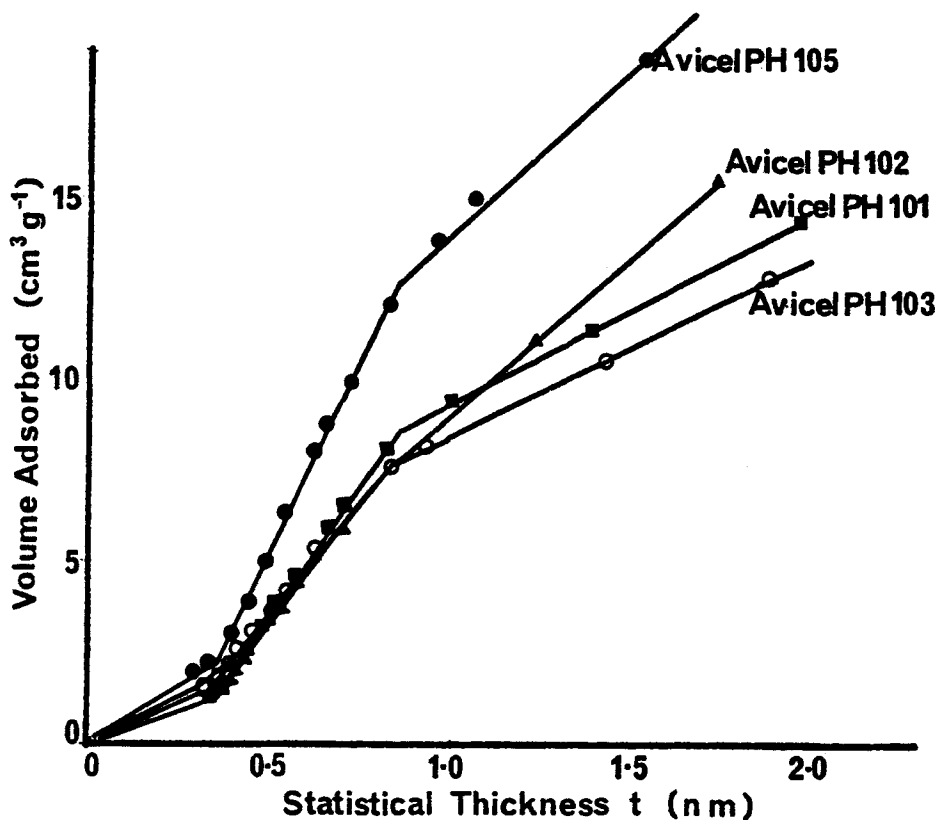


FIGURE 7.

Va-t isotherm for microcrystalline celluloses.

pore radius 'r' is given by:-

$$r = r_k + t_s \quad \text{----- (3)}$$

where $t_s = 4.02 \frac{V_a}{V_m}$

'V_a' being the volume of gas adsorbed at a given relative pressure, $\frac{P}{P_0}$, and 'V_m' being the volume adsorbed at monolayer coverage.

MARSHALL AND SIXSMITH

From these models, four were selected, namely those of Cranston and Inkley⁽¹²⁾ and Roberts I⁽¹³⁾ to represent cylindrical pore models, whilst those of Innes⁽¹⁴⁾ and Roberts II⁽¹³⁾ were taken as examples of parallel plate models. The pore size distribution derived from these analyses demonstrated that the microcrystalline celluloses studied had a large number of pores with radii from 1.25 to 3.0 nm, as shown in Figure 8, and were bimodal.

The mercury intrusion porosimetry experiments gave pore size distributions which showed modal values of 35 μm (PH 102), 20 μm (PH 101 and PH 103) and 5 μm (PH 105) as illustrated in Figure 3. It is possible to calculate surface areas from the porosimeter size distributions by graphical integration of the penetration volume against intrusion pressure plot according to the equation⁽¹⁵⁾

$$S = K \int_0^{V_{\text{max}}} P dV$$

where S = surface area $\text{m}^2 \text{g}^{-1}$

P = pressure N m^{-2}

dV = change in intrusion volume $\text{m}^3 \text{g}^{-1}$

This technique resulted in values much less than those obtained by gas adsorption, see Table II, suggesting that there is a large number of pores of radii less than the lower limit of the porosimeter (5.0 nm).

Examination of electronphotomicrographs of each of the samples at relatively low magnifications ($\times 500$) shows the presence of two types of particles, one rod-like, and the other an irregular mass. This could explain the change in slope of the

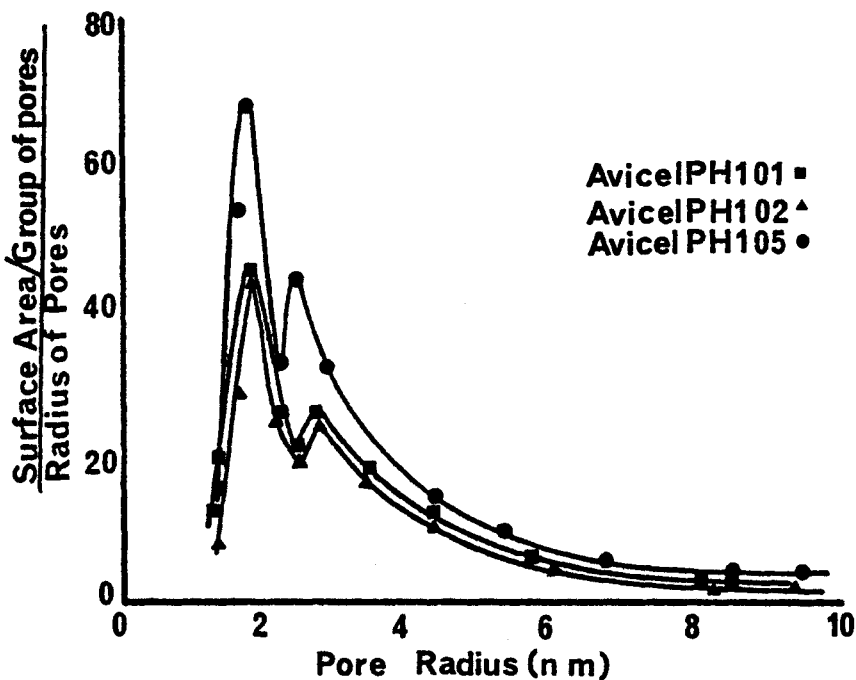


FIGURE 8.

Intraparticulate pore size distributions for microcrystalline celluloses.

distributions obtained by Coulter counter. Examination of fully hydrolysed samples at higher magnifications suggests that the material is composed of small fibrils with diameter between 10 and 15 nm and on some of the photographs these appear to be hollow as a central region of less electron density can be seen. The radius of this central axis approximates to that obtained for the majority of pores by gas adsorption measurements. Confirmation of this hollow core on untreated samples, i.e. not fully hydrolysed, was

TABLE II
Specific Surface Areas of Avicels

Avicel PH Grade	SURFACE AREA $m^2 g^{-1}$						
	Porosimetry	B.E.T.	Huttig	C & I	Roberts I	Innes	Roberts II
PH 102	1.26	10.0	10.5	14.2	13.4	10.2	10.0
PH 101	1.30	11.2	11.4	24.5	23.8	15.8	15.6
PH 103	1.36	11.4	11.5	21.3	20.8	14.0	13.7
PH 105	2.21	20.7	22.0	42.3	40.1	26.1	25.7

MICROCRYSTALLINE CELLULOSE. 1

obtained by the staining technique (Figure 5). It may be that the two types of particles originate during the manufacturing process, which is essentially one of partial acid hydrolysis, followed by spray drying of the washed slurry. Unhydrolysed cellulosic tissues might be expected to exhibit the rod-like appearance whilst the spray dried aggregates would be irregular.

The total porosity is made up of two components, the inter-particulate voids with size distributions as demonstrated by the mercury porosimetry results and intra-particulate pores with a modal radius value of about 2 nm. These results correlate well with the visual observations made by electron microscopy.

The results of the Heat of Adsorption experiments, Table III, using the flow microcalorimeter, confirm that the specific surface energies of the four grades, as measured by this technique,

TABLE III
Comparative Surface Energies of Avicels

Avicel PH Grade	Heat Liberated at Monolayer Coverage	
	$J g^{-1}$	$J m^{-2}$
PH 102	0.30	0.0287
PH 103	0.36	0.0287
PH 101	0.33	0.0285
PH 105	0.53	0.0285

MARSHALL AND SIXSMITH

are virtually identical and it seems reasonable to assume therefore that differences between the grades are not due to variation in this property.

CONCLUSION

The highly porous nature of these microcrystalline celluloses must contribute significantly to the rapid capillary uptake of water, leading to the rapid disintegration of tablets incorporating them. The relatively large surface areas will aid bonding and the microcalorimetry results show that the magnitude of the bonding forces is similar in all cases.

Further work is proceeding on consolidated microcrystalline celluloses in an endeavour to obtain more information about bonding mechanisms and studies of batch to batch variations are also in progress.

ACKNOWLEDGMENTS

The authors wish to acknowledge the advice and assistance of Dr. N. G. Stanley-Wood of the Postgraduate School of Powder Technology at Bradford in connection with the gas adsorption experiments and their interpretation.

We are also indebted to the F.M.C. Corpⁿ., Marcus Hook, U.S.A. for advice and the gift of samples of Avicel.

REFERENCES

1. C. D. Fox, M. D. Richman, G. E. Reier & R. F. Shangraw.
Drug & Cosmet. Ind., 92, 2, 161, 258 (1963).

MICROCRYSTALLINE CELLULOSE. 1

2. G. E. Reier & R. F. Shangraw. *J.Pharm.Sci.*, 55, 5, 510 (1966).
3. R. Huettenrauch, *Pharmazie*, 26, 645 (1971).
4. K. Marshall, D. Sixsmith & N. G. Stanley-Wood, *J.Pharm.Pharmac.*
24, Suppl., 138P (1972).
5. Avicel Product Bulletin PH-1, PH-4, F.M.C. Corporation, Pa.
6. Metric Units B.S.S. 4359 Part I (1969).
7. T. Allen & R. M. Patel, *J.Appl.Chem.*, 20, 165 (1970).
8. S. Brunauer, P. H. Emmett & E. Teller, *J.Am.Chem.Soc.*, 60,
1553 (1938).
9. G. F. Huttig, *Monatsch*, 78, 177 (1948).
10. B. C. Lippens & J.H. de Boer, *J. Catalysis*, 4, 319, 649 (1965).
11. W. T. Thompson, *Phil.Mag.*, 42, 448 (1871).
12. R. W. Cranston & F. A. Inkley, *Advances in Catalysis*, 9, 143
(1957).
13. B. F. Roberts, *J. Colloid & Interface Sci.*, 23, 266 (1967).
14. W. B. Innes, *Anal.Chem.*, 29, 1069 (1957).
15. H. M. Rootare & C. F. Prenzlou, *J.Phys.Chem.*, 71, 2733 (1967).